HHS Public Access

Author manuscript

Chem. Author manuscript; available in PMC 2021 July 09.

Published in final edited form as:

Chem. 2020 July 9; 6(7): 1634–1651. doi:10.1016/j.chempr.2020.06.019.

Porphyrinoid Drug Conjugates

Jonathan F. Arambula[1,2,*], **Jonathan L. Sessler**[1,*]

[1]Department of Chemistry, University of Texas at Austin, Austin, TX 78712-1224, USA

[2]OncoTEX, Inc, Austin, TX, USA

Abstract

Drawing inspiration from nature today remains a time-honored means of discovering the therapies of tomorrow. Porphyrins, the so-called “pigments of life” have played a key role in this effort due to their diverse and unique properties. They have seen use in a number of medically relevant applications, including the development of so-called drug conjugates wherein functionalization with other entities is used to improve efficacy while minimizing dose limiting side effects. In this Perspective, we highlight opportunities associated with newer, completely synthetic analogs of porphyrins, commonly referred to as porphyrinoids, as the basis for preparing drug conjugates. Many of the resulting systems show improved medicinal or site-localizing properties. As befits a Perspective of this type, our efforts to develop cancer-targeting, platinum-containing conjugates based on texaphyrins (a class of so-called “expanded porphyrins”) will receive particular emphasis; however, the promise inherent in this readily generalizable approach will also be illustrated briefly using two other common porphyrin analogs, namely the corroles (a “contracted porphyrin”) and porphycene (an “isomeric porphyrin”).

INTRODUCTION

Naturally occurring tetrapyrrolic systems, often referred to as the “pigments of life” by the late Sir Alan Battersby, include heme, chlorophyll, and coenzyme B_{12}, among other biological important cyclic and acyclic systems.[1] The colors have provided inspiration from well before the days of modern chemistry, as reflected in John Donne’s poetic line from his 1612 Progress of the Soul: “Why grass is green, or why our blood is red?”[2] They also influenced Richard Willstäter, who noted that it was the green color of nettles that inspired him to elucidate the structure of chlorophyll early in the 20th century.[3] That tour-de-force effort coupled with Hans Fischer’s work on the synthesis of protoporphyrin IX in the 1930s set the stage for continuing work on the synthesis of naturally occurring tetrapyrrolic pigments and, more recently, various synthetic analogs. This area has attracted the attention of some of the best preparative chemists on the planet and has done so for over 100 years. The central importance of tetrapyrrolic pigments to living systems and their amazing physical properties, from light absorption to catalysis and electron transfer, have likewise

* Correspondence: jfarambula@cm.utexas.edu (J.F.A.), sessler@cm.utexas.edu (J.L.S.).

DECLARATION OF INTERESTS

Many of the texaphyrin conjugates discussed in this perspective have been licensed by the University of Texas at Austin to OncoTEX, Inc. J.F.A. serves as vice president for research for OncoTEX. J.L.S. serves as a non-executive board member and scientific advisor to OncoTEX.

made them objects of interest to physical chemists, spectroscopists, biochemists, structural biologists, electrochemists, theorists, and many others. Depending on how wide one casts the net, the generalized area of naturally occurring pyrrole-based pigments has been recognized with no fewer than half a dozen Nobel Prizes,[4] including (1) Willstäter (Chemistry, 1915; for his research on plant pigments, especially chlorophyll); (2) Hans Fischer (Chemistry, 1930; in large measure for his synthesis of hemin); (3) Max Perutz and John Kendrew (Chemistry, 1962; for structures of hemoglobin and myoglobin); (4) Dorothy Hodgkin (Chemistry, 1964; for X-ray structural studies of biochemically important molecules including vitamin B_{12}); (5) Robert B. Woodward (Chemistry, 1965; for the art of organic synthesis including vitamin B_{12}); and (6) Johann Deisenhofer, Robert Huber, and Hartmut Michel (Chemistry, 1988; for determining the structure of the photosynthetic reaction center).

On a more pragmatic, if no less important level, naturally occurring tetrapyrrolic pigments and their semi-synthetic derivatives have been the basis of important drug development efforts. This is particularly true in the area of photodynamic therapy, where a combination of light and photosensitizer is used for medical benefit. Arguably, PDT dates to the pioneering studies of von Tappeiner and Jodlbauer, who in 1904 used fluorescent dyes applied topically in combination with light and oxygen to treat cancerous lesions.[5] Another famous early contribution was the self-experiment of Myer-Betz, who in 1913 found that hematoporphyrin promoted unusually severe sunburn.[6] However, it was Thomas J. Dougherty's pioneering work on hematoporphyrin derivative (Photofrin), leading to its FDA approval 1993 for bladder cancer that launched the field.[7,8] There are now several FDA-approved photosensitizers, including benzoporphyrin derivative monoacid ring A (BPD-MA, Visudyne) approved in 1999 for age-related macular degeneration in ophthalmology as well as other agents approved by other regulatory bodies. The field of PDT has been extensively reviewed.[9,10]

It is generally accepted that the first report of a pyrrolic macrocycle not containing the canonical four pyrroles found in porphyrin, chlorophyll, coenzyme B_{12}, and other naturally occurring pyrrolic pigments dates to 1966 when Woodward reported the isolation of the pentapyrrolic macrocycle sapphyrin as a reaction byproduct isolated during synthetic efforts directed toward vitamin B_{12}.[11,12] Since the mid-1980s, the chemistry of non-naturally occurring porphyrin analogs has all-but exploded. In fact, a special issue of Chemical Reviews on the topic published in 2017 ran to 1,200 printed pages.[13] Many of these efforts were focused on the biomedical potential of various synthetic porphyrin analogs ("porphyrinoids"), with corroles, porphycenes, and texaphyrins receiving particular attention in this context. These three porphyrinoids have also been subject to synthetic conjugation or modification to improve their "drug like" features and/or exploit their unique physiological properties.

The goal of this perspective is to highlight the biomedical potential of synthetic pyrrolic macrocycles, specifically those that contain central cavities that are "expanded," "contracted," or "isomeric" relative to porphyrin and that for the most part have no direct parallel in nature. The emphasis is placed on so-called conjugates wherein a central pyrrolic macrocyclic core is tethered to one or more entities so as to create a construct with better

perceived pharmaceutical properties. The treatment is meant to be illustrative, rather than comprehensive. It will thus focus on corroles, porphycenes, and texaphyrins, with particular emphasis being placed on the latter series of conjugates with which the authors have considerable personal familiarity.

CORROLES

The challenge inherent in the total synthesis of vitamin B_{12} spawned early efforts to create tetrapyrrolic macrocycles with the signature “missing” meso carbon found in the corrin core of this quintessential cobalt-containing cofactor. As part of a dedicated synthetic program targeting the preparation of porphyrin analogs, in 1964 A. W. Johnson detailed the discovery of a contracted tetrapyrrolic system known as corrole (Figure 1) as well as its first synthesis.[14] This macrocycle was arguably the first “contracted porphyrin” to be reported in the literature. However, studies of corroles were stymied by preparative difficulties, which precluded facile access. A break in this logjam came at the turn of the century with the reports by Gross and independently by Paolesse of high-yielding syntheses of corrole and complementary contributions from Gryko.[15–19] Since then, corrole systems have been extensively explored for their biological properties, mainly their use as potential scavengers of peroxynitrite,[20] agonists for photodynamic therapy,[21,22] and as high-affinity binding agents to G-quadraplexes.[23,24] These biological mechanisms have been proposed to have high utility in the treatment of cancer.

Similar to other porphyrins and porphyrinoids, the unique properties of corroles lie in their ability to coordinate transition and post-transition metals via N4 coordination. Considering that fully NH deprotonated corroles are tri-negative, complexation of a cation within the corrole core typically yields a metal center with a formal +3 charge. These systems were found to possess fluorescent properties and permit photo-induced inactivation of bacteria. To explore their medical utility, the overall charge of the system has been modulated,[25] and efforts have been made to increase their solubility[22] as a means to enhance drugability.

Protein Conjugates of Anionic Corroles

The most extensively studied corrole conjugate system involves the non-covalent coordination of the prophyrinoid core to protein carriers.[25,26,28] To facilitate this, Gross and collaborators prepared amphipolar systems containing hydrophilic sulfonic acid moieties on one single side of the macrocycle (Figure 2, compound 1). This electronic distribution favors the binding to carrier proteins as inferred from control studies wherein the sulfonic acid groups are symmetrically distributed around the core resulted in no cellular uptake. Early studies with complex 1 containing a gallium(III) (i.e., **1Ga**) metal center were found to undergo endocytosis into breast cancer cells, presumably abetted by coordination of **1Ga** to serum albumin. Additional cell uptake studies involved complexation of corroles to lipofectin, adenovirus serotype 5, and transferrin. It was later realized that despite the binding and formulation of corroles with transferrin, redistribution of corrole **1Ga** to human serum albumin took place in model studies.[26] Follow-up analyses in serum revealed binding of **1Ga** to 15% low-density lipoprotein (LDL) and 85% high-density lipoprotein (HDL). This line of investigation has culminated in the recent discovery of corrole-protein

conjugates based on the heregulin-targeted adenovirus fusion protein HerPBK10, a selective protein for the human epidermal growth factor receptor 2 (Her2). This bioconjugate, termed **HerGa**, was chosen for its specific receptor-targeting cell penetration (Figure 2). It also displayed high-affinity complexation to HerPBK10 and no redistribution in plasma.[27] Cellular studies revealed that **HerGa** bound selectively to cells expressing Her2 and is transported into cells via endosomes in breast cancer cell models. Subsequent fluorescent lifetime imaging *in vivo* in murine cancer models revealed clear tumor localization relative to organs and surrounding tissue (Figures 3A–3C).[28]

Anticancer mechanistic studies of **HerGa** revealed high anticancer potency in both melanoma (MDA-MB-435) and Her2 positive breast (MDA-MB-231) cancer cell models.[29] This was further evidenced in significant tumor growth delay *in vivo* (Figure 3D).[27] Unlike the positively charged corrole systems that show preference for G-quadraplexes to which they are bound strongly,[23,24] internalization of **HerGa** leads to the production of superoxide as well as the light-dependent production of singlet oxygen. Further cancer cell mechanistic studies with non-conjugated anionic corroles (e.g., **1**) revealed triggering of late M-phase cell-cycle arrest. While it is early days still, conjugates based on corrole appear to have a bright future as potential anticancer agents. In addition to this and outside the scope of this perspective, the ability to select the biological target or anticancer mechanism (e.g., targeting G-quadraplex versus reactive oxygen species [ROS] accentuation) by altering the charge justifies the further understanding of both as potential experimental therapeutics.

Porphycenes

A transformative milestone in the development porphyrin analog chemistry came with the late Emanuel Vogel's publication of porphycene in 1986.[30] Porphycenes constituted the first recognized porphyrin isomer, wherein the four pyrrole and meso carbon bridges are configured in a different spatial arrangement than in porphyrin (Figure 1). While a number of porphyrin isomers are now known, including N-confused porphyrins and their derivatives, porphycene remains the best studied in terms of its biomedical potential. It has been extensively explored as a photodynamic therapy sensitizer.[31] Moreover, in recent years, it has benefited from efforts to create drug conjugates to improve localization and therapeutic and pharmokinetic efficiency. However, at the time porphycenes were invented, the field of PDT sensitizers was less well advanced. Nevertheless, it was widely appreciated that a major limitation was that porphyrins, even aggregated forms, such as the inferred active components in Photofrin®, absorbed light in the blue-green portion of the visible spectrum where tissues were less transparent. Porphycene was found to absorb further to the red than porphyrin leading to its exploration as a photosensitizer. One porphycene that proved particularly promising in this regard was 9-acetoxy2,7,12,17-tetrakis-(μ-methoxyethyl)-porphycene **2** (Figure 4A). It was evaluated in the 1990s by Glaxo Dermatology (GlaxoWellcome, NC, USA) and Cytopharm (Calif, USA) as a PDT sensitizer for dermatological applications against psoriasis vulgaris and superficial non-melanoma skin cancer.

Considerable effort has been devoted to improving the inherent features of porphycenes by creating conjugates. Among the early conjugates to be reported were polylysine porphycene

systems (e.g., **3**) that were studied for the light-induced inactivation of microbial pathogens.[32,33] In recent years, several new porphycene conjugates based on clinically approved antibiotics have been reported. One such example contains gentamicin as the active payload. Gentamicin is an aminoglycoside used for the treatment of a broad range of systemic bacterial infections (conjugate **4**, Figure 4A).[34] Further studies illustrated the selective photoinactivation of *E. coli* and *S. aureus* by **4** relative to controls (Figures 4B and 4C). This promising result is considered an augury of even more impressive microbial eradication efforts that are likely yet to come.

TEXAPHYRINS

Texaphyrin—A Tumor-Localizing Anticancer Agent

Following Woodward's 1966 report of sapphyrin, sporadic, albeit seminal, efforts were devoted to the synthesis of larger porphyrinoids. However, the term "expanded porphyrin" and the utility of this class of molecules as ligands dates only to 1988 when we reported the synthesis of a class of pentaaza Schiff base expanded porphyrins known as texaphyrins.[35,36] Chemically, texaphyrins are characterized by the presence of an inner coordination core that is roughly 20% larger than that present in porphyrins. They also have a formal charge of 1– (relative to 2– for porphyrin/porphycene, and 3– for corroles). Early on, they were found to form stable 1:1 complexes with a wide variety of metal cations, particularly with those of the trivalent lanthanide series.[35] This finding, coupled with an appreciation that metallotexaphyrins were both easy to reduce in a ligand-centered manner and could be reoxidized reversibly by air to produce ROS[37,38] and, in the case of the diamagnetic complexes, good photosensitizers,[39] led to an appreciation that they might have a role to play as potential drug leads. Two leads, namely motexafin gadolinium (**MGd**, cf. Figure 5A) and motexafin lutetium (**MLu**), were selected for clinical development.[40] As the result of considerable effort, involving the Sessler group at the University of Texas at Austin, researchers at Pharmacyclics, (acquired by AbbVie in 2015), and a cadre of dedicated clinicians, it is now appreciated that **MGd** has several attributes that are rather unique in the context of anticancer drug development. These include: (1) a novel mechanism of action that leads to apoptosis without disrupting DNA;[41] (2) an ability to localize within cancerous lesions (i.e., distributions of greater than 9:1 relative to surrounding tissues as evidenced by MRI enhancements, fluorescence bio-imaging, and radiolabeling *in vivo*); and (3) a high relaxivity that permits easy visualization via magnetic resonance imaging (MRI) (Figure 5B).[42–44] Furthermore, **MGd** is well tolerated, and multiple-dose regimens have been administered to a large number of patients at the 5 mg/kg level without any clinically significant adverse effects (i.e., no grade 3 or 4 toxicities).[45,46] This combination of features is unique to the texaphyrins and makes them, as a class, attractive for use in creating tumor-targeting conjugates.[47–49] For a more specific recent review on texaphyrins and their broad application, see Zheng et al.[50]

Early examples were focused on developing the synthetic methods needed to prepare several proof-of-concept texaphyrin-based conjugates.[51] As **MGd** was being clinically pursued as a tumor-localizing adjuvant to radiation therapy for the treatment of metastatic lung cancer, novel conjugate designs encompassed known cancer therapies, such as platinum,

anthracyclines, antimetabolites, and radiation sensitizers. These early designs focused on robust, non-labile linkers connecting the texaphyrin and chemotherapy subunits. The rationale for this was based on the need for robust conjugation to avoid or minimize chemical degradation in plasma. Little biological data were reported for these early complexes.

However, one report describing the amide (robust, **5**) and ester (labile, **6**) conjugation of methotrexate revealed that it was sub-optimal to have linkers of either extreme. For example, **6** was found to possess a better anticancer potency *in vitro* than **5**. However, **6** was found to be more hydrolytically labile relative to the stable **5**, thus, suggesting the degradation of **6** in plasma. These results support the desire for a tumor-specific controlled release (Figure 6A).[52] This was evidenced by cell proliferation studies in which A549 human lung cancer cells were non-responsive to exposure by **5** but responsive to treatments with labile **6** (Figure 6B). Based on this early work, it was also inferred that effective intracellular release of an appended therapeutic would prove essential were the putative conjugate to achieve the design objective of targeted drug delivery. Early fluorescence studies with **MGd** revealed organelle specific localization to lysosomes, mitochondria, and endoplasmic reticulum.[53] Taking this into account, ensuing generations of texaphyrin conjugates were designed to contain active therapeutics attached through readily cleaved linkers. In doing so, the therapeutic would undergo a release (via controlled release or hydrolytic cleavage) in the subcellular environment in which it would be most effective. For a variety of reasons, the bulk of this effort has focused on texaphyrin-platinum conjugates.

Texaphyrin-Platinum

Cisplatin and carboplatin (Figure 7) are two of the most important antitumor agents for the treatment of cancer, which has long been recognized as the second leading cause of death behind heart disease in the United States.[54] While considered successful for the treatment of particular cancer types, such as testicular cancer with cisplatin, their clinical utility is limited. In the particular case of ovarian cancer, the leading cause of death for gynecological cancers, their use as a front-line therapy in combination with taxol translates to an overall 45%–48% 5-year survival rate.[54–56] However, roughly 60% of the total ovarian cancer population is diagnosed with advanced cancer. Here, the clinical utility of platinum becomes limited by intrinsic or acquired resistance and is reflected in a 5-year survival rate of less than 30%.[56] Recent clinical trials that focused on addressing Pt-resistant ovarian cancer with chemotherapies or biologicals have demonstrated little success.[57–60] The biochemical and pharmacologic mechanisms of Pt-resistance (e.g., decreased drug uptake, increased glutathione, and increased DNA adduct repair) are well established.[55] In an effort to overcome these challenges, texaphyrin conjugates containing platinum were explored.

Early designs were focused on the preparation of texaphyrin-platinum conjugates containing amine-type carrier ligands. It was rationalized that in doing so, the putative increase in intracellular platinum would result in a greater number of Pt-DNA adducts analogous to those formed by cisplatin or carboplatin. The design expectation was that the resulting increase in DNA damage would then overwhelm the cancer cell driving it toward apoptosis. To this end, cisplatin texaphyrin conjugate **7** containing a malonate linker for Pt(II) chelation

was produced.[61] It was found that its anticancer cytotoxicity *in vitro* was similar to that of control carboplatin in platinum-sensitive A2780 ovarian cancer cells and twice as potent in the isogenic platinum-resistant strain 2780CP/Cl-16 (Table 1). Further mechanistic studies revealed two key benefits when the platinum was administered as conjugate **7** relative to control carboplatin: (1) the cancer cell uptake and resulting DNA platination was greater and (2) the uptake and DNA platination was equal across both sensitive and resistant cell lines (Figure 8).[62] This finding provided an important early hint that texaphyrins could be used as carriers to overcome pharmacologic resistance mechanisms involving platinum uptake. However, analysis of the DNA damage tolerance (i.e., ability of the cancer cell line to tolerate the damage) led to the conclusion that the increase in intracellular Pt provided by conjugate **7** would likely not be sufficient to overcome all major forms of platinum drug resistance.[62]

In parallel to the above work on **7**, efforts were made to explore texaphyrin-platinum conjugates that undergo controlled reductive release upon reaching the tumor-reductive micro environment. This was done through incorporation of a platinum with a higher oxidation state (i.e., Pt(IV) center, complex 8).[63] These systems were also found to be potent against cancer cell models *in vitro* and illustrated enhanced intracellular uptake relative to platinum controls. Unique to this system, the reductive release of cisplatin from conjugate **8** could be controlled by exposure to a reducing metabolite (i.e., glutathione) or light. This allowed for the controlled platination of DNA in model studies (Figure 9). While the finding that conjugate **8** allowed (1) pharmacological resistance mechanisms to be overcome as reflected in good cellular uptake of Pt in both sensitive and resistant cells and (2) incorporation of tumor-specific controlled release represented key advances, it was evident that the inability to overcome molecular mechanisms of platinum resistance (see discussion below) would require further fine-tuning of the design.

Molecular mechanisms of platinum drug resistance co-exist with pharmacological mechanisms of resistance and present treatment-limiting barriers to the effective application of both cisplatin and carboplatin in the clinic. Among the known molecular mechanisms of Pt-resistance, the most formidable involves loss of function for the tumor suppressor p53 as the result of selection pressures.[64] This is particularly problematic in the case of cisplatin and carboplatin as ovarian cancers harboring mutant p53 are widespread and display attenuated responses.[65,66] However, one must be cautious in oversimplifying p53 status (and patient prognosis) as being either wild type (WT) or mutant. It was illustrated by yeast functional assays (FASAY) of over 2,000 p53 mutations that 64% of the mutants retained WT activity.[67] On the other hand, cisplatin resistance in mutant p53 cells maintaining WT-p53 activity was found to be significantly greater (2- to 3-fold) than in mutant p53 cells not possessing WT-p53 activity.[64] It is now appreciated that DNA damage by cisplatin or carboplatin is mediated, in part, by Chk2 kinases, which are often downregulated in platinum-resistant cancers and lead to a lack of post-translational modification of p53 for its functional activation. In contrast, DNA damage by the third FDA platinum drug, oxaliplatin, and similar platinum agents is mediated by MEK1/2 kinases.[68] This alteration in signal transduction by oxaliplatin is directly related to the di-aminocyclohexane (DACH) carrier ligand as illustrated by oxaliplatin being distinct and non-cross resistant (unlike cisplatin or

carboplatin) in several p53 dysfunctional ovarian cancer cell lines.[68] We therefore turned our attention to the development of texaphyrin-platinum conjugates containing the DACH carrier ligand. Below, we detail efforts to create texaphyrin-platinum conjugates based on a DACH chelating moiety. The goal in creating such systems was to retain the pharmacological resistance benefits seen in the earlier conjugates, while creating lead systems capable of reactivating dormant p53 activity.

Our initial design along these lines is embodied in conjugate **9** (Figure 7).[69] Gratifyingly, and in contrast to the texaphyrin-platinum conjugates containing ammonium carrier ligands, conjugate **7** was found to be highly potent in both the WT A2780 and platinum-resistant 2780CP/Cl-16 ovarian cancer cell lines with no cross resistance being observed (Table 1). These favorable findings were attributed to the ability of conjugate **9** to overcome both pharmacologic and molecular mechanisms of platinum resistance. Upon further inspection, it was found that an equal amount of platinum (as conjugate **9**) was taken into both platinum-sensitive and platinum-resistant cancer cells (Figure 8). Of particular significance was that the level of uptake in 2780CP/Cl-16 cells was similar to the level of uptake in A2780 cells treated with cisplatin. Investigations into the ability of **9** to overcome p53-mediated molecular mechanisms of resistance were also conducted. Western blot and flow cytometric analyses revealed that conjugate **9** induces apoptosis via the activation of p53, its subsequent phosphorylation, and the downstream transactivation of p21. Unfortunately, a combination of limited plasma stability and formulation issues prevented in-depth analyses of conjugate **9** *in vivo*.

Efforts to maintain the core design (i.e., texaphyrin + DACH-Pt) but improve both the solubility and plasma stability resulted in the creation of the Pt(IV) prodrug conjugate **10**.[70] The general design of **10** was inspired by our findings that **MGd** could mediate the intermolecular reduction of Pt(IV) to Pt(II) in the presence of cancer cells.[71] Initial conjugate optimization efforts were focused on varying the Pt(IV) axial ligands so as to optimize the reduction potential of the Pt(IV) center (and hence, the key release features of the conjugate). It was found that an acetate ligand provided the best balance between reductive stability and anticancer potency. Conjugate **10** was also found to maintain the same *in vitro* potency as conjugate **9** (cf. Table 1), enhance the *in vivo* uptake, and re-activate p53 (cf. Figure 10). Conjugate **10** also displayed enhanced stability in plasma and was found to be easily formulated in 5% dextrose/water.

The *in vivo* efficacy of conjugate **10** was explored in nude mice bearing subcutaneous xenografts.[70] It was found to be well tolerated when administered intravenously at the 70 mg/kg dose level. Efficacy studies in mice bearing A549 human lung cancer xenografts revealed a statistically significant delay in tumor growth (61% tumor growth inhibition [TGI]) in mice administered prodrug conjugate **10**. In contrast, conjugate **9** produced no statistically meaningful growth inhibition (Figure 11A). We speculate that this contrast reflects, in part, differences in plasma stability. Prodrug conjugate **10** was also evaluated in platinum-resistant patient-derived xenograft (PDX) efficacy models.[70] In many cases, treatment with **10** provided a statistically significant benefit relative to the control platinum drug used clinically for that particular cancer type. For example, an evaluation of CTG-0253, a platinum-resistant ovarian cancer PDX model, resulted in 100% TGI and increase in

survival in mice treated with **10**, whereas treatment with carboplatin (the standard of care platinum for ovarian cancer) resulted in no discernable anticancer activity.

Efforts were then made to evaluate the biodistribution of conjugate **10** after tail vein administration in non-tumor bearing mice.[70] It was found that the tissue biodistribution of platinum (as **10**) differed from that seen for oxaliplatin. Of particular note was the finding that a larger amount of platinum were found in the liver relative to the kidney as compared with the clinically approved platinum drugs. This redirection in the tissue biodistribution is thought due to the texaphyrin core whose main metabolic pathway is hepatic, presumably mediated via cytochrome P450 reductase.[72] Enhanced plasma retention was also observed, which was ascribed to the fact that conjugate **10** binds well to serum albumin.[70] Of particular interest is that **10** retained its anticancer activity as an albumin complex. This stands in contrast to oxaliplatin whose activity was found to be attenuated by the apparent irreversible binding to albumin.[70]

Studies were also conducted to evaluate the tolerability and pathology of conjugate **10** in CD1 mice. Comparisons were made to oxaliplatin at equimolar platinum doses (1 dose/day on days 1, 5, 9, and 13). The efficacious and “high dose with acceptable weight loss” doses (HD-AWL) of **10**, 70 mg/kg/dose (corresponding on a per mole basis to platinum concentrations of 16.2 mg/kg/dose in oxaliplatin), and the efficacious and approximate MTD of oxaliplatin, 6 mg/kg/dose in this animal model (which would correspond to a per mole platinum concentration of 25.9 mg/kg/dose of **10**), were tested. Mice treated with 70 mg/kg/dose of **10** experienced recoverable minor weight loss over the treatment period (Table 2) with no notable adverse clinical symptoms being observed. Mice treated with an equimolar platinum dose of oxaliplatin (16.2 mg/kg/dose) experienced significant body weight loss and severe adverse clinical effects with 3 of the 8 mice requiring early euthanasia. Hematology, clinical pathology, and blood chemistry revealed minor adverse events in mice treated with the HD-AWL of **10**. Bone marrow atrophy was the most clinically significant finding, albeit not at a level that was considered likely to engender concern.

Texaphyrin-Doxorubicin

The chemotherapeutic class of anthracyclines are a mainstay in current therapeutic regimes due to their broad applicability. Originally extracted from the bacterium *Streptomyces*, the extended aromatic system within the members of this class acts as a DNA intercalator, which in turn inhibits the activity of topoisomerase II.[73,74] To date, the anthracyclines daunorubicin and doxorubicin have received FDA approval for the treatment of soft and solid tumors, respectively. Recognizing that the first generation Gd(III) and Lu(III) texaphyrins localizes to solid tumors, an effort was made to prepare texaphyrin-doxorubicin conjugates based on the **MGd** core.

From a conceptual standpoint, a labile linker was viewed as essential for the development of a doxorubicin-texaphyrin conjugate.[75,76] This is because doxorubicin can only elicit its beneficial cytotoxic effects once it enters the nucleus, where it inhibits topoisomerase II. In contrast, prior confocal microscopic studies of texaphyrins revealed localization to lysosomes, the mitochondria, and the endoplasmic reticulum, as noted above.[53] The

development of an effective doxorubicin-based texaphyrin conjugate would thus provide support for the notion that a cleavable linker had indeed been implemented into the conjugate design.

While texaphyrin-doxorubicin conjugates containing acid labile hydrazone linkers have been synthesized and mechanistically explored *in vitro*,[75] the most in-depth analysis involved a conjugate containing a disulfide linker.[76] Based on prior work with fluorescent probes,[75,78] it was expected that in the presence of glutathione (typically present at higher relative concentrations in cancer cells) cleavage would occur to release the active doxorubicin payload as in conjugate **11** (Figure 12). This was not expected to be the case for the C–C linked control, **12**. Conjugate **11** proved to be highly stable under physiological conditions. However, upon the addition of glutathione, time-dependent doxorubicin release was observed. This was evidenced by an increase in the doxorubicin-based fluorescence (Figure 13A) and confirmed by high-pressure liquid chromatography (HPLC) analysis. Fluorescence microscopy experiments were used to visualize uptake of **11** (and subsequent intracellular release of doxorubicin) into KB and CT26 liver cancer cells (Figure 13B). Both conjugates **11** and **12** were assessed for their ability to inhibit cell proliferation in CT-25 liver cancer cells (Figure 13C). Greater potency was observed in the case of **11**, containing the degradable disulfide linker, than in its more robust analog **12**. Such a finding is consistent with the idea that in the case of the disulfide conjugate **11**, free doxorubicin is released, which then migrates to the nucleus.

For *in vivo* tests, folate nanoliposomal formulations of **11** were made up and tested in xenograft and metastatic liver cancer models in immunocompromised mice. Xenograft-bearing mice (n = 3 treated intravenously [i.v.] with **11**) produced readily visualized tumor-localized MR images (Figure 13D) and a slowed tumor growth (assessed by tumor volume) relative to saline control over a 3-week monitoring period (Figure 13F). MRI analysis of tumor growth in the metastatic liver cancer model revealed a significant reduction in tumor burden relative to controls (Figure 13F). Moreover, increased survival was seen with **11** relative to saline and controls. Unfortunately, the benefit, although statistically significant, did not rise to a level that would justify further preclinical development. Thus, current efforts are being made to fine-tune the linker and optimize the controlled release of this and other active pharmaceutical payloads. To the extent this is achieved it is expected to enhance the power and potency of the texaphyrin-based conjugate drug deliver strategy whose rich potential is embodied in the Pt(IV) drug conjugate **10**.

CONCLUSIONS

As fully synthetic, and often privileged, macrocycles, porphyrin analogs have a rich future in the contest of drug conjugate design. In this perspective, we have highlighted only a few examples within the full lexicon of what can be imagined. There are now dozens, likely hundreds, of expanded, contracted, isomeric porphyrins known in the literature. It is expected that each particular chemical entity will bring to this drug design area its own individual strengths and weaknesses. These attributes would include, but are not limited to, unique redox, metal coordination, optical, and structural features. The ability to choose which of these features leads to the best drug candidate and optimize accordingly provides a

versatility that may not be replicated in the case of nature's all-important but still limited set of tetrapyrrolic macrocycles. In favorable instances, more than one ancillary entity could be attached allowing both druggability and potency to be fine-tuned. We thus predict that this is an area of drug discovery and development with a particular rich future.

ACKNOWLEDGMENT

This work was supported by the National Institutes of Health (grant R01 CA68682) and the Robert A. Welch Foundation (F-0018).

REFERENCES

1. Battersby AR (2000). Tetrapyrroles: the pigments of life. Nat. Prod. Rep. 17, 507–526. [PubMed: 11152419]
2. Chambers EK, ed. (1896). The Poems of John Donne (Lawrence & Bullen).
3. Robinson R (1953). Richard Willstätter. 1872–1942. Obit. Not. Fell. R. Soc. 8, 609–634.
4. Sen DJ (2017). Nobel Laureates of Chemistry from 1901 to Present Millennium (Lambert Academic Publishing).
5. von Tappeiner H, and Jodlbaur A (1904). Ueber wirking der photodynamichen (fluorescierenden) stoffe auf protozoan und enzyme. Dtsch. Arch. Klin. Med. 80, 427–487.
6. Friedrich M-B (1913). Untersuchungen über die biologische (photodynamische) wirkung des hämatoporphyrins und anderer derivate des blut-und gallenfarbstoffs. Dtsch. Arch. Klin. Med. 112, 476–503.
7. Dougherty TJ, Gomer CJ, Henderson BW, Jori G, Kessel D, Korbelik M, Moan J, and Peng Q (1998). Photodynamic therapy. J. Natl. Cancer Inst. 90, 889–905. [PubMed: 9637138]
8. Macdonald IJ, and Dougherty TJ (2001). Basic principles of photodynamic therapy. J. Porphyrins Phthalocyanines 05, 105–129.
9. Almeida-Marrero V, van de Winckel E, Anaya-Plaza E, Torres T, and de la Escosura A (2018). Porphyrinoid biohybrid materials as an emerging toolbox for biomedical light management. Chem. Soc. Rev. 47, 7369–7400. [PubMed: 30152500]
10. Baskaran R, Lee J, and Yang SG (2018). Clinical development of photodynamic agents and therapeutic applications. Biomater. Res. 22, 25. [PubMed: 30275968]
11. Woodward RB (1966) Aromaticity: An International Symposium Held at Sheffield on 6th–8th July (Chemical Society).
12. Bauer VJ, Clive DLJ, Dolphin D, Paine JB, Harris FL, King MM, Loder J, Wang SWC, and Woodward RB (1983). Sapphyrins: novel aromatic pentapyrrolic macrocycles. J. Am. Chem. Soc. 105, 6429–6436.
13. Sessler JL, Gross Z, and Furuta H (2017). Introduction: expanded, contracted, and isomeric porphyrins. Chem. Rev. 117, 2201–2202. [PubMed: 28222607]
14. Johnson AW, and Kay IT (1965). 306. Corroles. Part I. Synthesis. J. Chem. Soc. 1965, 1620–1629.
15. Gross Z, Galili N, and Saltsman I (1999). The first direct synthesis of corroles from pyrrole. Angew. Chem. Int. Ed. Engl. 38, 1427–1429. [PubMed: 29711568]
16. Paolesse R, Licoccia S, Bandoli G, Dolmella A, and Boschi T (1994). First direct synthesis of a corrole ring from a monopyrrolic precursor. Crystal and molecular sructure of (triphenylphosphine)(5,10,15-triphenyl-2,3,7,8,12,13,17,18-octamethylcorrolato) cobalt(III)-dichloromethane. Inorg. Chem. 33, 1171–1176.
17. Paolesse R, Mini S, Sagone F, Boschi T, Jaquinod L, Nurco DJ, and Smith KM (1999). 5,10,15-triphenylcorrole: a product from a modified Rothemund reaction. Chem. Commun. 1999, 1307–1308.
18. Gryko DT (2002). Recent advances in the synthesis of corroles and core-modified corroles. Eur. J. Org. Chem. 2002, 1735–1743.

19. Koszarna B., and Gryko DT. (2006). Efficient synthesis of meso-substituted corroles in a H2O–MeOH mixture. J. Org. Chem. 71, 3707–3717. [PubMed: 16674040]
20. Mahammed A, and Gross Z (2006). Iron and manganese corroles are potent catalysts for the decomposition of peroxynitrite. Angew. Chem. Int. Ed. Engl. 45, 6544–6547. [PubMed: 16960906]
21. Hwang JY, Lubow DJ, Chu D, Sims J, Alonso-Valenteen F, Gray HB, Gross Z, Farkas DL, and Medina-Kauwe LK (2012). Photoexcitation of tumor-targeted corroles induces singlet oxygen-mediated augmentation of cytotoxicity. J. Control. Release 163, 368–373. [PubMed: 23041277]
22. Barata JFB, Zamarrón A, Neves MGPMS, Faustino MAF, Tomé AC, Cavaleiro JAS, Röder B, Juarranz Á, and Sanz-Rodríguez F (2015). Photodynamic effects induced by mesotris(pentafluorophenyl)corrole and its cyclodextrin conjugates on cytoskeletal components of HeLa cells. Eur. J. Med. Chem. 92, 135–144. [PubMed: 25549553]
23. Fu B, Huang J, Ren L, Weng X, Zhou Y, Du Y, Wu X, Zhou X, and Yang G (2007). Cationic corrole derivatives: a new family of G-quadruplex inducing and stabilizing ligands†. Chem. Commun. 2007, 3264–3266.
24. Fu B., Zhang D., Weng X., Zhang M., Ma H., Ma Y, and Zhou X. (2008). Cationic metal–corrole complexes: design, synthesis, and properties of guanine-quadruplex stabilizers. Chemistry 14, 9431–9441. [PubMed: 18752229]
25. Teo RD, Hwang JY, Termini J, Gross Z, and Gray HB (2017). Fighting cancer with corroles. Chem. Rev. 117, 2711–2729. [PubMed: 27759377]
26. Haber A, Agadjanian H, Medina-Kauwe LK, and Gross Z (2008). Corroles that bind with high affinity to both apo and holo transferrin. J. Inorg. Biochem. 102, 446–457. [PubMed: 18180041]
27. Agadjanian H, Ma J, Rentsendorj A, Valluripalli V, Hwang JY, Mahammed A, Farkas DL, Gray HB, Gross Z, and Medina-Kauwe LK (2009). Tumor detection and elimination by a targeted gallium corrole. Proc. Natl. Acad. Sci. USA 106, 6105–6110. [PubMed: 19342490]
28. Hwang JY, Wachsmann-Hogiu S, Ramanujan VK, Ljubimova J, Gross Z, Gray HB, Medina-Kauwe LK, and Farkas DL (2012). A multimode optical imaging system for preclinical applications in vivo: technology development, multiscale imaging, and chemotherapy assessment. Mol. Imaging Biol. 14, 431–442. [PubMed: 21874388]
29. Agadjanian H, Weaver JJ, Mahammed A, Rentsendorj A, Bass S, Kim J, Dmochowski IJ, Margalit R, Gray HB, Gross Z, and Medina-Kauwe LK (2006). Specific delivery of corroles to cells via noncovalent conjugates with viral proteins. Pharm. Res. 23, 367–377. [PubMed: 16411149]
30. Vogel E, Köcher M, Schmickler H, and Lex J (1986). Porphycene-a novel porphin isomer. Angew. Chem. Int. Ed. Engl. 25, 257–259.
31. Stockert JC, Cañete M, Juarranz A, Villanueva A, Horobin RW, Borrell JI, Teixidó J, and Nonell S (2007). Porphycenes: facts and prospects in photodynamic therapy of cancer. Curr. Med. Chem. 14, 997–1026. [PubMed: 17439399]
32. Polo L, Segalla A, Bertoloni G, Jori G, Schaffner K, and Reddi E (2000). Polylysine–porphycene conjugates as efficient photosensitizers for the inactivation of microbial pathogens. J. Photochem. Photobiol B Biol. 59, 152–158.
33. Lauro FM, Pretto P, Covolo L, Jori G, and Bertoloni G (2002). Photoinactivation of bacterial strains involved in periodontal diseases sensitized by porphycene–polylysine conjugates. Photochem. Photobiol Sci. 1, 468–470. [PubMed: 12659156]
34. Nieves I, Hally C, Viappiani C, Agut M, and Nonell S (2020). A porphycene-gentamicin conjugate for enhanced photodynamic inactivation of bacteria. Bioorg. Chem. 97, 103661. [PubMed: 32086054]
35. Sessler JL, Hemmi G, Mody TD, Murai T, Burrell A, and Young SW (1994). Texaphyrins: synthesis and applications. Acc. Chem. Res. 27, 43–50.
36. Sessler JL, Mody TD, Hemmi GW, and Lynch V (1993). Synthesis and structural characterization of lanthanide(III) texaphyrins. Inorg. Chem. 32, 3175–3187.
37. Maiya BG, Harriman A, Sessler JL, Hemmi G, Murai T, and Mallouk TE (1989). Ground- and excited-state spectral and redox properties of cadmium(II) texaphyrin. J. Phys. Chem. 93, 8111–8115.

38. Sessler JL, Tvermoes NA, Guldi DM, Mody TD, and Allen WE (1999). One-electron reduction and oxidation studies of the radiation sensitizer gadolinium(III) texaphyrin (PCI-0120) and other water soluble metallotexaphyrins. J. Phys. Chem. A 103, 787–794.
39. Harriman A, Maiya BG, Murai T, Hemmi G, Sessler JL, and Mallouk TE (1989). Metallotexaphyrins: a new family of photosensitisers for efficient generation of singlet oxygen. J. Chem. Soc. Chem. Commun. 1989, 314–316.
40. Sessler JL, and Miller RA (2000). Texaphyrins: new drugs with diverse clinical applications in radiation and photodynamic therapy. Biochem. Pharmacol. 59, 733–739. [PubMed: 10718331]
41. Magda D (2005). Gadolinium (III) texaphyrin (Xcytrin): a new class of redox acitve drug leads In Medicinal Inorganic Chemistry, Sessler JL, Doctrow S, and Lippard SJ, eds. (Oxford University Press).
42. Miller RA, Woodburn K, Fan Q, Renschler MF, Sessler JL, and Koutcher JA (1999). In vivo animal studies with gadolinium (III) texaphyrin as a radiation enhancer. Int. J. Radiat. Oncol. Biol. Phys. 45, 981–989. [PubMed: 10571206]
43. Mehta MP, and Khuntia D (2005). Current strategies in whole-brain radiation therapy for brain metastases. Neurosurgery 57, S33–S44. [PubMed: 16237287]
44. Mehta MP, Shapiro WR, Glantz MJ, Patchell RA, Weitzner MA, Meyers CA, Schultz CJ, Roa WH, Leibenhaut M, Ford J, et al. (2002). Lead-in phase to randomized trial of motexafin gadolinium and whole-brain radiation for patients With brain metastases: centralized assessment of magnetic resonance imaging, neurocognitive, and neurologic end points. J. Clin. Oncol. 20, 3445–3453. [PubMed: 12177105]
45. Mehta MP, Shapiro WR, Phan SC, Gervais R, Carrie C, Chabot P, Patchell RA, Glantz MJ, Recht L, Langer C, et al. (2009). Motexafin gadolinium combined with prompt whole brain radiotherapy prolongs time to neurologic progression in non-small-cell lung cancer patients With brain metastases: results of a phase III trial. Int. J. Radiat. Oncol. Biol. Phys. 73, 1069–1076. [PubMed: 18977094]
46. Mehta MP, Rodrigus P, Terhaard CHJ, Rao A, Suh J, Roa W, Souhami L, Bezjak A, Leibenhaut M, Komaki R, et al. (2003). Survival and neurologic outcomes in a randomized trial of motexafin gadolinium and whole-brain radiation therapy in brain metastases. J. Clin. Oncol. 21, 2529–2536. [PubMed: 12829672]
47. Sessler JL (2016). Texaphyrins In Macrocyclic and Supramolecular Chemistry, Izatt RM, ed. (John Wiley & Sons), pp. 309–324.
48. Arambula JF, Preihs C, Borthwick D, Magda D, and Sessler JL (2011). Texaphyrins: tumor localizing redox active expanded porphyrins. Anti Cancer Agents Med. Chem. 11, 222–232.
49. Preihs C, Arambula JF, Magda D, Jeong H, Yoo D, Cheon J, Siddik ZH, and Sessler JL (2013). Recent developments in texaphyrin chemistry and drug discovery. Inorg. Chem. 52, 12184–12192. [PubMed: 23557113]
50. Keca JM, and Zheng G (2019). Texaphyrin: from molecule to nanoparticle. Coord. Chem. Rev. 379, 133–146.
51. Magda DJ, Wang Z, Gerasimchuk N, Wei W-H, Anzenbacher P, and Sessler JL (2004). Synthesis of texaphyrin conjugates. Pure Appl. Chem. 76, 365–374.
52. Wei WH, Fountain M, Magda D, Wang Z, Lecane P, Mesfin M, Miles D, and Sessler JL (2005). Gadolinium texaphyrin–methotrexate conjugates. Towards improved cancer chemotherapeutic agents. Org. Biomol. Chem. 3, 3290–3296. [PubMed: 16132091]
53. Woodburn KW (2001). Intracellular localization of the radiation enhancer motexafin gadolinium using interferometric Fourier fluorescence microscopy. J. Pharmacol. Exp. Ther. 297, 888–894. [PubMed: 11356908]
54. Siegel RL, Miller KD, and Jemal A (2020). Cancer statistics, 2020. CA Cancer J. Clin. 70, 7–30. [PubMed: 31912902]
55. Siddik ZH (2003). Cisplatin: mode of cytotoxic action and molecular basis of resistance. Oncogene 22, 7265–7279. [PubMed: 14576837]
56. American Cancer Society (2020). Cancer facts & figures 2020 (American Cancer Society), pp. 1–70.

57. Bozkaya Y, Doğan M, Umut Erdem G, Tulunay G, Uncu H, Arık Z, Demirci U, Yazıcı O, and Zengin N (2017). Effectiveness of low-dose oral etoposide treatment in patients with recurrent and platinum-resistant epithelial ovarian cancer. J Obstet Gynaecol 37, 649–654. [PubMed: 28325092]
58. Pujade-Lauraine E, Hilpert F, Weber B, Reuss A, Poveda A, Kristensen G, Sorio R, Vergote I, Witteveen P, Bamias A, et al. (2014). Bevacizumab combined with chemotherapy for platinum-resistant recurrent ovarian cancer: the Aurelia open-label randomized phase III trial. J. Clin. Oncol. 32, 1302–1308. [PubMed: 24637997]
59. McClung EC, and Wenham RM (2016). Profile of bevacizumab in the treatment of platinum-resistant ovarian cancer: current perspectives. Int. J. Womens Health 8, 59–75. [PubMed: 27051317]
60. Marth C, Vergote I, Scambia G, Oberaigner W, Clamp A, Berger R, Kurzeder C, Colombo N, Vuylsteke P, Lorusso D, et al. (2017). ENGOT-ov-6/TRINOVA-2: randomised, double-blind, phase 3 study of pegylated liposomal doxorubicin plus trebananib or placebo in women with recurrent partially platinum-sensitive or resistant ovarian cancer. Eur. J. Cancer 70, 111–121. [PubMed: 27914241]
61. Arambula JF, Sessler JL, Fountain ME, Wei W-H, Magda D, and Siddik ZH (2009). Gadolinium texaphyrin (Gd-Tex)-malonato-platinum conjugates: synthesis and comparison with carboplatin in normal and Pt-resistant cell lines. Dalton Trans 2009, 10834–10840.
62. Arambula JF, Sessler JL, and Siddik ZH (2011). Overcoming biochemical pharmacologic mechanisms of platinum resistance with a texaphyrin-platinum conjugate. Bioorg. Med. Chem. Lett. 21, 1701–1705. [PubMed: 21345675]
63. Thiabaud G, Arambula JF, Siddik ZH, and Sessler JL (2014). Photoinduced reduction of PtIV within an anti-proliferative PtIV-texaphyrin conjugate. Chem. Eur. J. 20, 8942–8947. [PubMed: 24961491]
64. Mehta K, and Siddik ZH (2009). Drug resistance and the tumor supressor p53: the paradox of wild-type genotype in chemorefractory cancers In Drug Resistance in Cancer Cells (Springer Science).
65. Bast RC Jr., Hennessy B, and Mills GB (2009). The biology of ovarian cancer: new opportunities for translation. Nat. Rev. Cancer 9, 415–428. [PubMed: 19461667]
66. Ozols RF (2006). Challenges for chemotherapy in ovarian cancer. Ann. Oncol. 17, v181–v187. [PubMed: 16807453]
67. Kato S, Han SY, Liu W, Otsuka K, Shibata H, Kanamaru R, and Ishioka C (2003). Understanding the function-structure and function-mutation relationships of p53 tumor suppressor protein by high-resolution missense mutation analysis. Proc. Natl. Acad. Sci. USA 100, 8424–8429. [PubMed: 12826609]
68. Bhatt M, Ivan C, Xie X, and Siddik ZH (2016). Drug-dependent functionalization of wild-type and mutant p53 in cisplatin-resistant human ovarian tumor cells 8, 10905–10918.
69. Arambula JF, Sessler JL, and Siddik ZH (2012). A texaphyrin-oxaliplatin conjugate that overcomes both pharmacologic and molecular mechanisms of cisplatin resistance in cancer cells. Medchemcomm 3, 1275–1281. [PubMed: 23936624]
70. Thiabaud G, He G, Sen S, Shelton KA, Baze WB, Segura L, Alaniz J, Munoz Macias R, Lyness G, Watts AB, et al. (2020). Oxaliplatin Pt(IV) prodrugs conjugated to gadolinium-texaphyrin as potential antitumor agents. Proc. Natl. Acad. Sci. USA 117, 7021–7029. [PubMed: 32179677]
71. Thiabaud G, McCall R, He G, Arambula JF, Siddik ZH, and Sessler JL (2016). Activation of platinum(IV) prodrugs by motexafin gadolinium as a redox mediator. Angew. Chem. Int. Ed. Engl. 55, 12626–12631. [PubMed: 27377046]
72. Mani C, Upadhyay S, Lacy S, Boswell GW, and Miles DR (2005). Reductase-mediated metabolism of motexafin gadolinium (Xcytrin) in rat and human liver subcellular fractions and purified enzyme preparations. J. Pharm. Sci. 94, 559–570. [PubMed: 15666291]
73. Fujiwara A, Hoshino T, and Westley JW (1985). Anthracycline antibiotics. Crit. Rev. Biotechnol. 3, 133–157.
74. Tacar O, Sriamornsak P, and Dass CR (2013). Doxorubicin: an update on anticancer molecular action, toxicity and novel drug delivery systems. J. Pharm. Pharmacol. 65, 157–170. [PubMed: 23278683]

75. Lee MH, Kim EJ, Lee H, Park SY, Hong KS, Kim JS, and Sessler JL (2016). Acid-triggered release of doxorubicin from a hydrazone-linked Gd(3+)-texaphyrin conjugate. Chem. Commun. (Camb.) 52, 10551–10554. [PubMed: 27492744]

76. Lee MH, Kim EJ, Lee H, Kim HM, Chang MJ, Park SY, Hong KS, Kim JS, and Sessler JL (2016). Liposomal texaphyrin theranostics for metastatic liver cancer. J. Am. Chem. Soc. 138, 16380–16387. [PubMed: 27998081]

77. Lee MH, Kim JY, Han JH, Bhuniya S, Sessler JL, Kang C, and Kim JS (2012). Direct fluorescence monitoring of the delivery and cellular uptake of a cancer-targeted RGD peptide-appended naphthalimide theragnostic prodrug. J. Am. Chem. Soc. 134, 12668–12674. [PubMed: 22642558]

78. Lee MH, Jeon HM, Han JH, Park N, Kang C, Sessler JL, and Kim JS (2014). Toward a chemical marker for inflammatory disease: a fluorescent probe for membrane-localized thioredoxin. J. Am. Chem. Soc. 136, 8430–8437. [PubMed: 24840911]

The Bigger Picture

Challenges and opportunities

- Future porphyrinoid-conjugates should incorporate multi-functional or multi-modal capabilities so as to achieve their full potential as a unique class within experimental therapeutics
- The diversification in the mechanisms of action that are possible with porphyrinoid drug conjugates should be exploited. Exploring points of variability involving the porphyrinoid (i.e., metal and overall charge) and the conjugated motif (i.e., therapeutic, protein, etc.) will further diversify a class of drugs with unique mechanistic attributes
- The attenuation or refinement of pharmacological properties (i.e., pharmacokinetics, disease localization, toxicity profile, etc.) is broadly needed within this class of experimental therapeutics to expand the number of candidates that warrant development

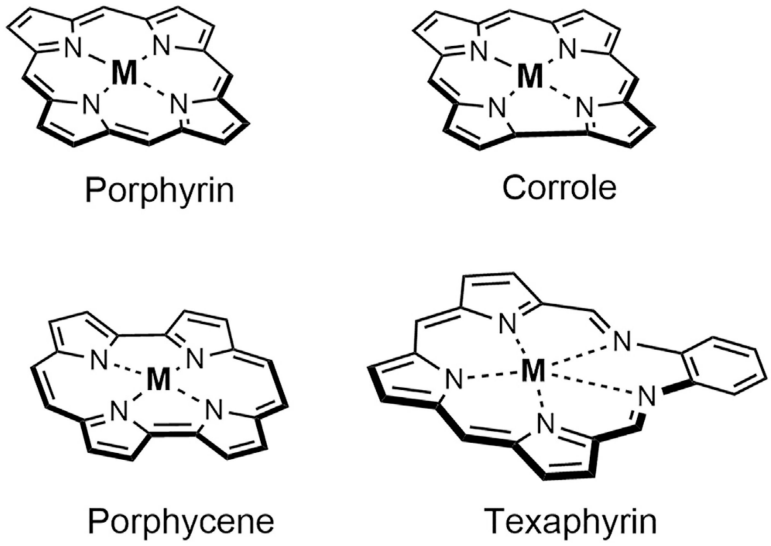

Figure 1. General Core Structures of Natural Porphyrin and Porphryrinoids Corrole, Porphycene, and Texaphyrin

M, metal. or H.

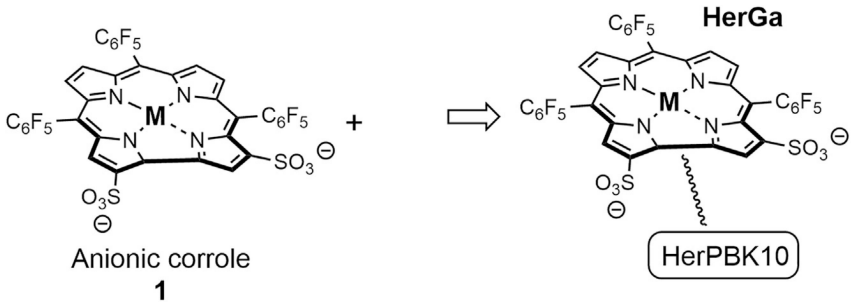

Figure 2.

Anionic Corrole System 1 Coordinating to HerPBK10 to Generate the Corrole-Protein Conjugate HerGa Containing a Gallium Metal Center

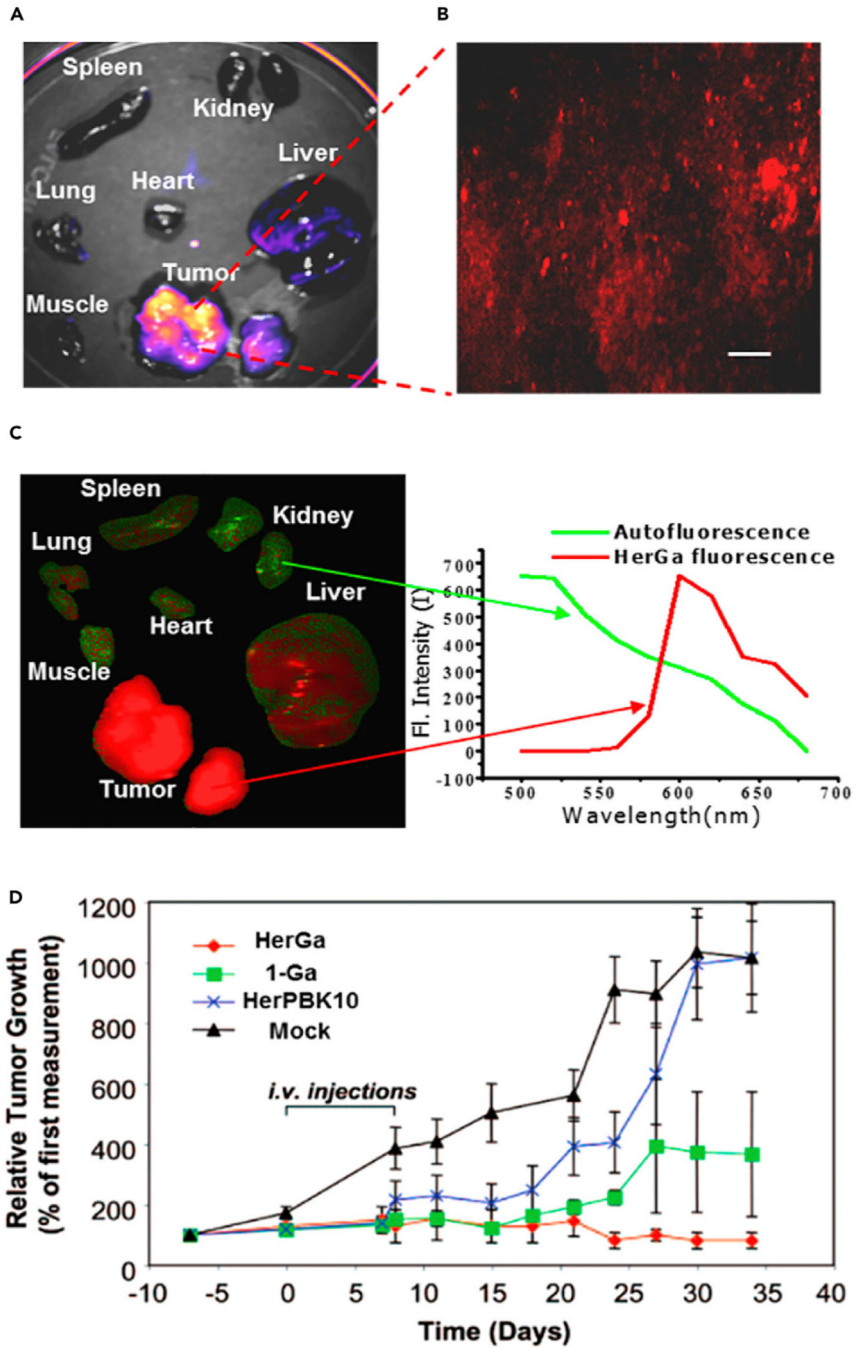

Figure 3. *In Vivo* Tumor Localization and Efficacy of HerGA

(A–C) *In vivo* fluorescent images of tumor and surrounding tissue and organs from mice treated with **HerGa**. Copyright 2017 American Chemical Society.[24]

(D) Efficacy study of **HerGA**, corrole **1Ga**, and controls in mice bearing Her2-positive human breast cancer xenografts. Copyright 2009 National Academy of Sciences.[26]

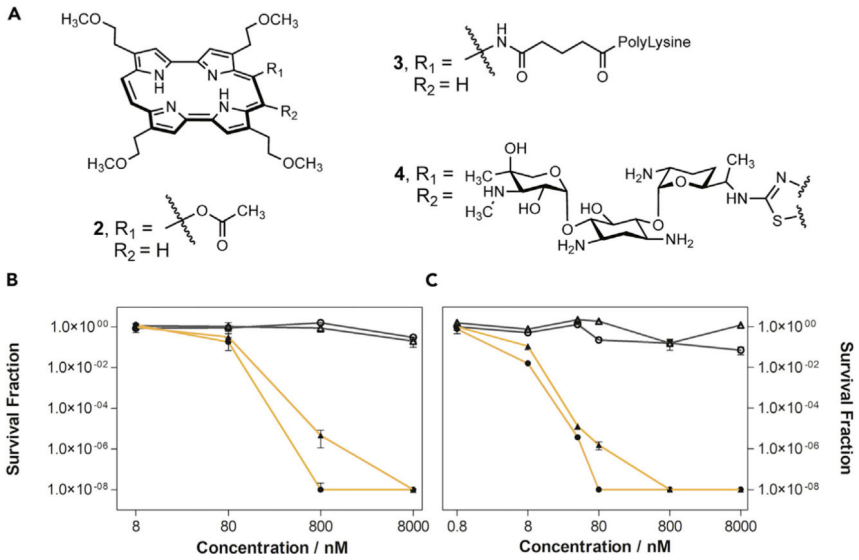

Figure 4. Corrole and Corrole Conjugate Systems as Antibiotics

(A) Porphycene 2, porphycene-polylysine conjugate **3**, and porphycene-gentamicin conjugate **4**. (B and C) (B) *E. coli* and (C) *S. aureus* photoinactivation studies with 4 upon red light irradiation (λ = 638 ± 9 nm). Light doses: 30 J·cm^{-2} (filled triangles), 45 J·cm^{-2} (filled circles). Working concentrations: 0.8 (only for *S. aureus*), 8, 80, 800, and 8,000 nM. Incubation time: 2 h. Dark controls are represented with gray empty symbols. Reprinted with permission by Nonell, et al., Copyright 2020 Elsevier.[33]

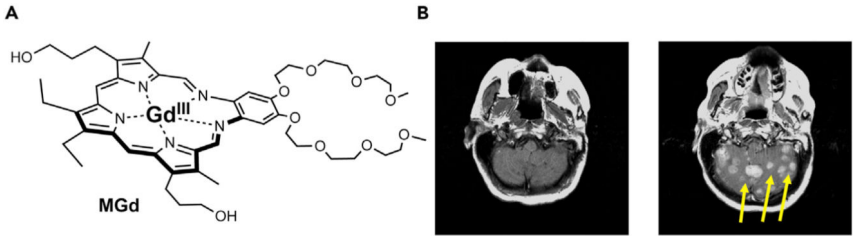

Figure 5. MRI Capabilities of Gadolidium-Bound Texaphyrins

(A) **MGd**.

(B) T1-weighted brain MRI scans of a patient with non-small-cell lung cancer: Left, noncontrast scan at baseline; right, noncontrast scan after 10 daily administration of **MGd** at of 5 mg/kg/day.

Copyright 2016 Wiley.[46]

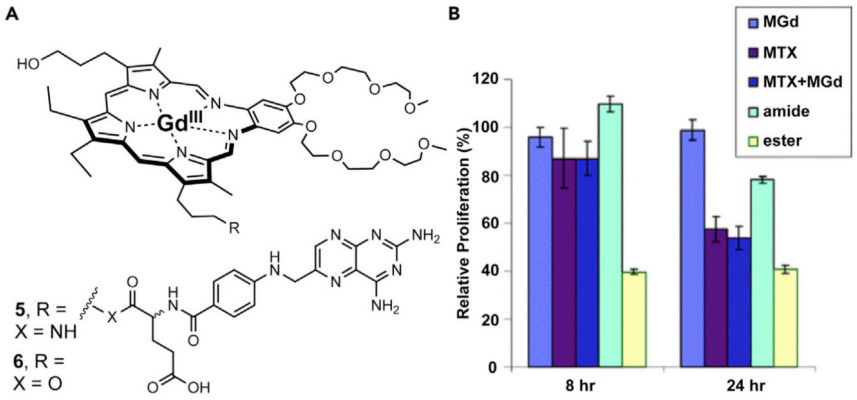

Figure 6. ***In Vitro*** **Anticancer Activity of MGd and Texaphyrin Methotrexate Conjugates**

(A) **MGd** and texaphyrin methotrexate (MTX) conjugates containing robust amide (**5**) and labile ester (**6**) linkers.

(B) Relative cell proliferation data in A549 human lung cancer cells treated with respective complexes including amide conjugate **5** and ester conjugate **6**. Copyright 2005 Royal Society of Chemistry.[49]

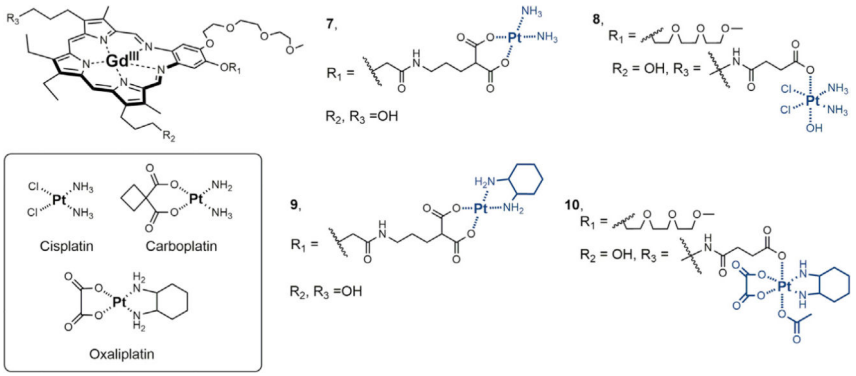

Figure 7.
Cisplatin, Carboplatin, Oxaliplatin, and Various Texaphyrin-Platinum Conjugates

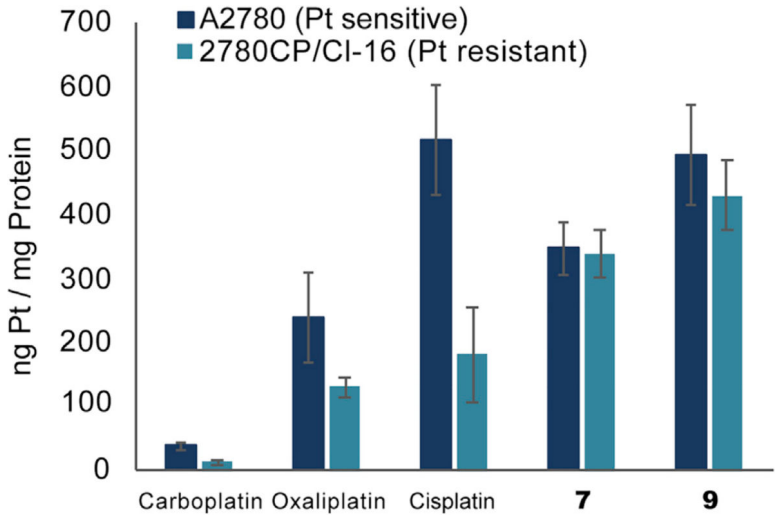

Figure 8. Intracellular Platinum Uptake in A2780 and 2780CP Ovarian Cancer Cells Treated with the Respective Platinum Agent

Quantitative platinum levels were determined by flameless atomic absorption spectrometry of cellular digests.

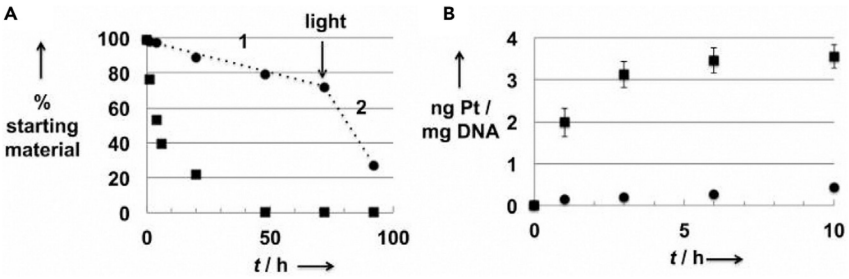

Figure 9. Controlled Platinum Release and DNA Binding of Conjugate 10

(A) Stability (RP-HPLC analysis) of **10** in PBS solution in the dark (black circles) or exposed to laboratory light (black squares), the designation 1 indicates the hydrolysis phase (absence of light), while the 2 indicates the phase corresponding to light exposure.

(B) Quantification by FAAS (Pt) and by NanoDrop (DNA) of the number of Pt-DNA adducts formed after reaction of **10** with DNA in the dark (black circles) or exposed to natural light (black squares).

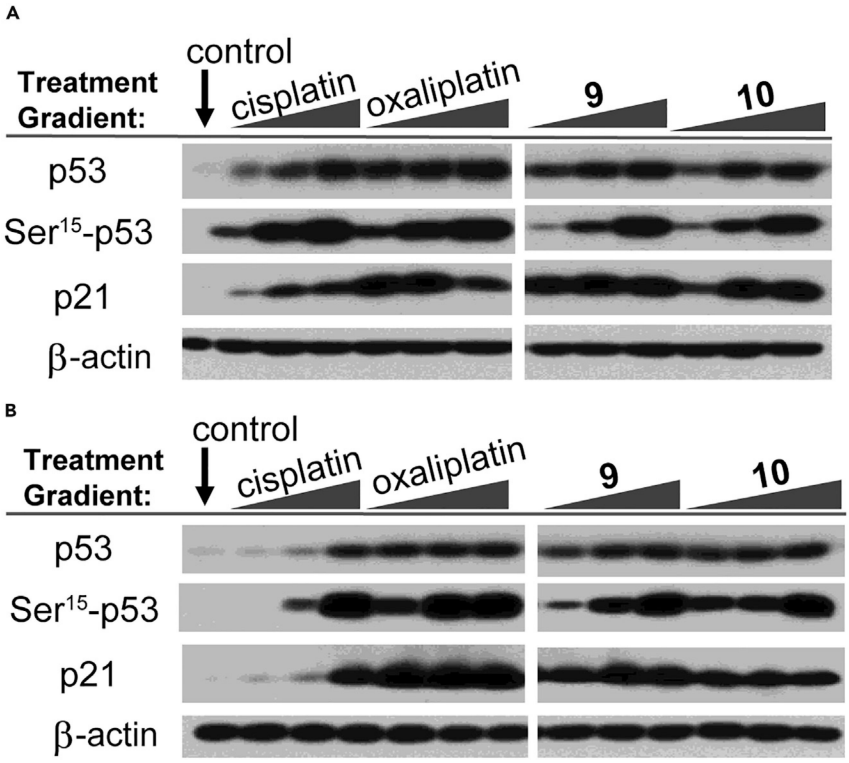

Figure 10. P53 Pathway Activation via Western Blot Analysis

(A and B) (A) A2780 cisplatin-sensitive and (B) 2780CP/Cl-16 cisplatin-resistant ovarian cancer cells treated with variable concentrations of platinum agent.

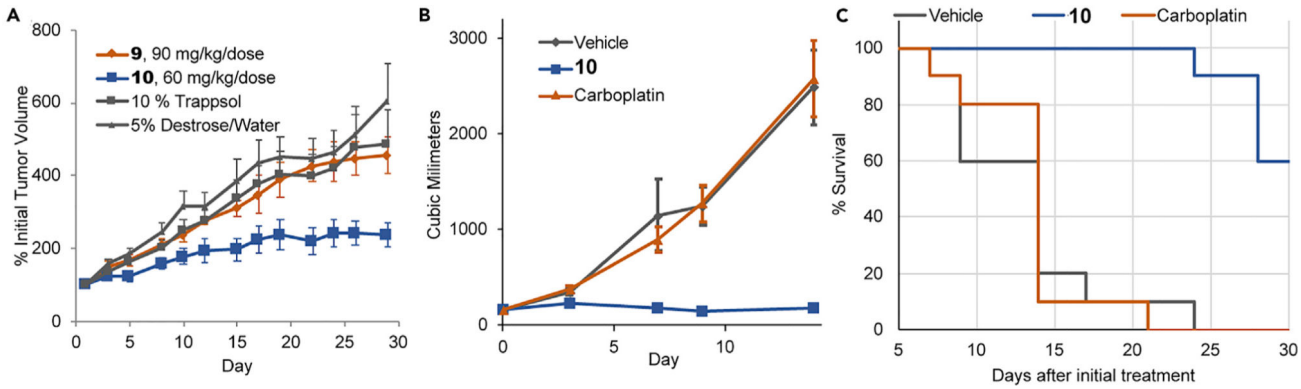

Figure 11. ***In Vivo*** **Efficacy and Survival Studies in Mice Treated with Texaphyrin-Platinum Conjugates**

(A) Subcutaneous A549 xenograft study in nude mice treated with **9**, **10**, and relative vehicle controls.

(B) Efficacy study of nude mice bearing platinum-resistant ovarian tumors (model CTG-0253), which were treated i.v. with vehicle, carboplatin, and conjugate **10**.

(C) Resulting Kaplan-Meier survival plot of mice of study described in Figure 12B.

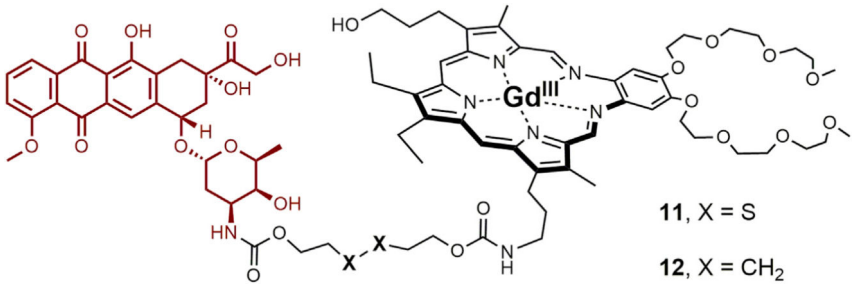

Figure 12.

Texaphyrin-Doxorubicin Conjugate Containing Reductively Labile Disulfide Linker (11) and Control Conjugate 12, Containing a Robust Non-labile Linker

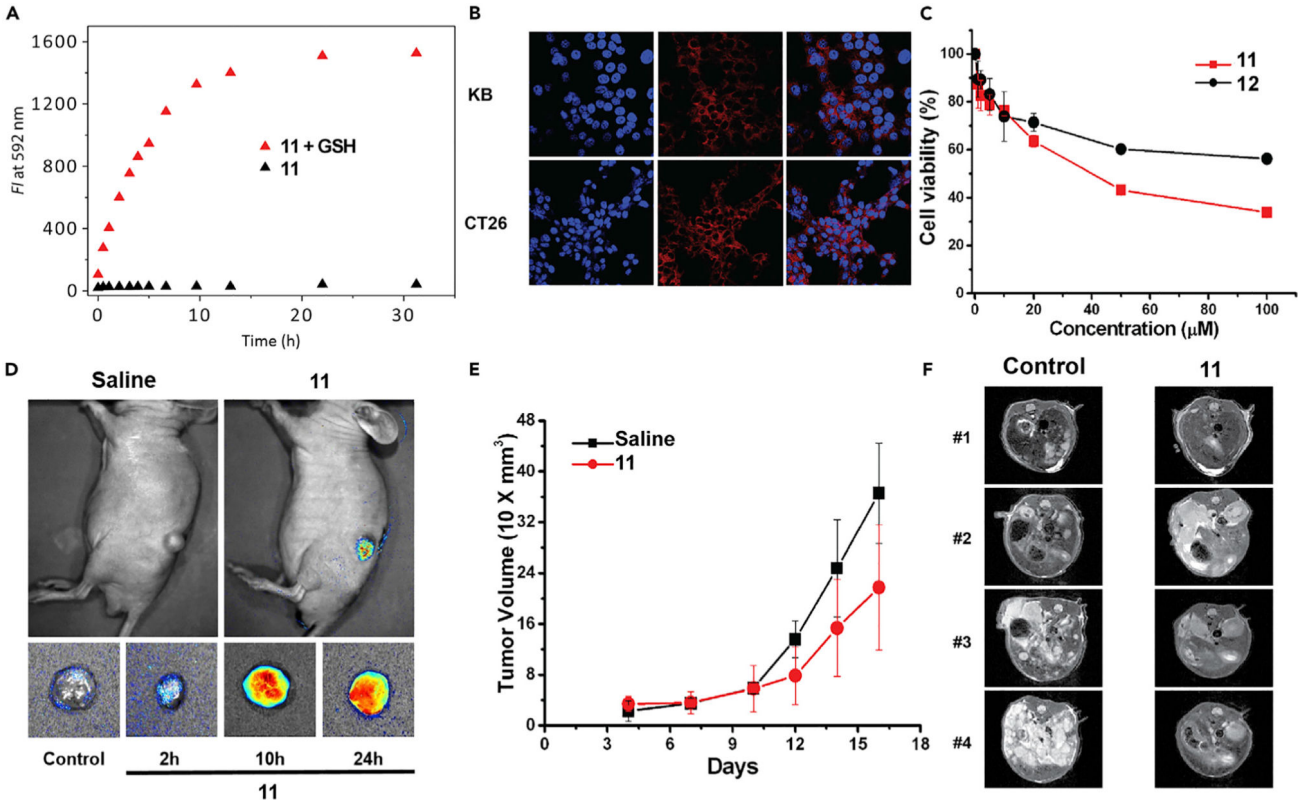

Figure 13. ***In Vitro*** **and** ***In Vivo*** **Studies Involving Conjugate 11**

(A) Fluorescence emission of GSH-dependent doxorubicin release of **11**.

(B) Fluorescence microscopy illustrating uptake of **11** into KB and CT26 cell lines.

(C) Enhanced antiproliferative effect seen for **11** (containing a GSH-trigged cleavable linker) relative to its non-degradable congener **12** possessing a robust C–C tether in CT-25 liver cancer cell lines.

(D) Subcutaneous xenograft cancer model. MR imaging of tumor using **11**.

(E) Efficacy study with **11**, which was injected at the 2.5 mg/kg dose (i.v.) every other day (four times total) starting on day 4 post-tumor inoculation.

(F) Metastatic liver cancer model. **11** was injected as in (E) starting on day 3. Monitoring was by TY2-weighted MRI imaging on day 15.

Table 1.

IC_{50} Values of Pt Complexes in A2780 and 2780CP/Cl-16 Ovarian Human Cancer Cell Lines

Complex	**IC_{50} (*u*M)**		**Resistance Factor**
	A2780[a]	**2780CP/Cl-16**	**2780CP/A2780**
Cisplatin	0.3	7.1	23.7
Carboplatin	1.3	27	20.8
Oxaliplatin	0.15	0.3	2.0
7	1.6	17	10.6
8	1.3	10.7	8.2
9	0.55	0.65	1.2
10	0.55	0.65	1.2

[a]A2780 and 2780CP/Cl-16 ovarian cancer cell lines represent an isogenic human cancer cell pair that displays multidrug resistance due, in part, to the inability of mutant p53 activation by cisplatin and carboplatin.

Table 2.

Dosing and Body Weight Change of CD1 Mice Treated with 10 and Oxaliplatin

Drug	Dose, mg/kg per Dose	Pt per Dose, Nmol	BW Change Day 14, %	BW Change Day 28, %
Vehicle	Vehicle	N/A	+3.5%	NA
10	70 (HD-AWL)	41	−7.5%	+1.0%
Oxaliplatin	16.2	41	−16.5%[a]	N/A
10	25.9	15	+6.4%	+5.8%
Oxaliplatin	6 (MTD)	15	+8.9%	+14.8%

[a]40% of mice not evaluated as they were removed from study due to adverse drug effects.